Development of an Indoor Photovoltaic Energy Harvesting Module for Autonomous Sensors in Building Air Quality Applications

Xicai Yue, *Senior Member, IEEE*, Matthias Kauer, *Senior Member, IEEE*, Mathieu Bellanger, Oliver Beard, Mike Brownlow, Des Gibson, Caspar Clark, Calum MacGregor, and Shigeng Song

***Abstract*—A 50 mm × 20 mm × 15 mm indoor photovoltaic (PV) energy harvesting power module (IPEHPM) has been developed for powering an Internet of Things (IoT) sensor node containing a low-power CO_2 sensor for automatic building ventilation. It is composed of a high efficiency PV energy harvesting module and a supercapacitor to produce 3.6–4.2 V output voltage with 100 mA pulse current for up to 600 ms. Storage efficiency analysis and storage efficiency tests of the IPEHPM have demonstrated that with the adopted simple power management scheme, which exempts the commonly used power management blocks of the voltage regulator and the maximum power point tracking to save power, 88.7% average storage efficiency has been achieved at 200 lux. With the newly established PV powering model, the power consumption requirements of an IoT node can be directly converted into the illumination requirements of the PV energy harvester, making the IPEHPM easy to use. IPEHPM powered IoT experiments with a low-power CO_2 gas sensor have demonstrated that the IPEHPM is suitable for IoT-based building ventilation applications, where the CO_2 concentration level is measured every 150 s at the indoor lighting condition down to 200 lux.**

***Index Terms*—Energy harvesting, Internet of Things (IoT), low-power CO_2 sensor, maximum power point tracking (MPPT), photovoltaic (PV), power management, self-discharge, supercapacitor.**

I. Introduction

WIRELESS sensor networks (WSNs) and the Internet of Things (IoT) will soon be used widely in our daily lives. Market intelligence currently predicts that the volume of IoT connected devices is in the range of 45 billion by 2020 [1], with sensors accounting for more than 60% of devices [2].

A major issue for autonomous wireless devices is still their need for a connected power source and often this power source is provided in the form of disposable batteries. With the emergence of new low-power sensor solutions the network communications landscape is rapidly changing from wired to wireless whereby all devices are becoming connected, interoperable, and require rapid deployment.

There is a need to implement new powering strategies for such autonomous sensors, widen technology awareness and increase uptake by eliminating battery change as a major operational and environmental issue [3]. The same analysis has identified relevant energy harvesting applications in sectors, such as building automation, agriculture, health and medical and process monitoring. Insufficient power available for the application was one of the main reasons identified for not adopting energy harvesting in these sectors.

A typical example is the use of WSN's in buildings for enhanced control and management of air handling systems, reducing building energy consumption and enhancing building air quality to ensure occupants well-being [4]–[7]. Buildings are responsible for at least 40% of the world's total energy consumption with 96% of our existing building stock currently with limited or no effective building energy management systems in place [8]. Smart air quality control in buildings can be achieved via automated control of air handling systems based on the real-time measurement of air CO_2 concentration, temperature, and humidity, implemented using the IoT, with energy savings up to 25%. Since building environmental parameters do not change quickly, each sensor node in the IoT only needs to work in active mode periodically for sensing, processing, and communication. The power hungry active mode has a relatively short time period, such as in the order of ms at the power consumption in mW, while the ultralow power consumption sleeping mode is relatively long, such as in order of minutes at the power consumption in μW. Therefore, the average power consumption of an IoT-based sensor node is much lower than the power consumption in active mode, making it possible to power an IoT-based sensor node using ambient energy harvesting components, such as photovoltaic (PV) energy harvesters, where

Manuscript received February 10, 2017; revised May 24, 2017 and July 24, 2017; accepted September 11, 2017. Date of publication September 20, 2017; date of current version December 11, 2017. This work was supported by the Innovate U.K. under Contract 102156. *(Corresponding author: Xicai Yue.)*

X. Yue is with the Faculty of Environment and Technology, Department of Engineering Design and Mathematics, University of the West of England, Bristol BS16 1QY, U.K. (e-mail: alex.yue@uwe.ac.uk).

M. Kauer and M. Bellanger are with the Sharp Laboratories of Europe, Oxford OX4 4GB, U.K., and also with the Sharp Innovation Centre, Lightricity Ltd., Oxford OX4 4GB, U.K.

O. Beard and M. Brownlow are with the Sharp Laboratories of Europe, Oxford OX4 4GB, U.K.

D. Gibson is with the Gas Sensing Solutions, Glasgow G68 9HQ, U.K., and also with the Institute of Thin Films, Sensors and Imaging, University of the West of Scotland, Scottish Universities Physics Alliance, Paisley PA1 2BE, U.K. (e-mail: des.gibson@uws.ac.uk).

C. Clark and C. MacGregor are with Gas Sensing Solutions, Glasgow G68 9HQ, U.K.

S. Song is with the Institute of Thin Films, Sensors and Imaging, University of the West of Scotland, Scottish Universities Physics Alliance, Paisley PA1 2BE, U.K.

Digital Object Identifier 10.1109/JIOT.2017.2754981

energy harvested during the sensor node's sleep period can be continuously accumulated in energy storage components (such as a supercapacitor) so that a high power pulse can be produced for the measuring and data sending period. The long lifetime of energy harvesting and storage components (such as millions of recharge circles for a supercapacitor) enables the IoT-based sensor node to be powered using energy harvesting in a "fit and forget" manner without worrying about battery replacement.

Attempts at integrating PV cells, power management circuits and even storage together to provide a fully integrated PV energy harvesting power chip which finally leads to self-powered IoT systems have been reported [9]–[11]. However, due to the chip size restriction, the total harvested energy is limited so it is suitable for some ultralow power applications but is not generic for powering a low-power IoT-based sensor node.

The power consumption of the IoT-based sensor node has been lowered thanks to the development in low-power electronics and sensor technologies. However, it is difficult to further reduce the total power consumption of the IoT node due to the relatively higher power requirements for wireless data communication. The low illumination indoor conditions which restrict the amount of the harvested PV energy, makes the case of powering indoor IoT sensor node more challenging. As a result, there is no indoor PV energy harvesting powered wireless sensor node existing for CO_2 concentration measurements.

This paper presents the development of an indoor PV energy harvesting power module (IPEHPM) for wireless sensor nodes. The project utilizes a low-power consumption autonomous CO_2, temperature, and humidity sensor and its associated signal conditioning circuits [12] from Gas Sensing Solutions Ltd. (GSS, Glasgow, U.K.) together with extra IoT node circuits, powered using the newly developed IPEHPM. The rest of this paper is organized as follows. Section II describes the development of the IPEHPM, including specifications, components details, the new power management scheme without using the maximum power point tracking (MPPT) to save power, storage efficiency analysis for the new power management scheme, and the newly proposed powering model to link the IoT application's power consumption requirements into the illumination conditions of the IPEHPM. Section III describes the testing of the IPENPM, including storage efficiency tests, parameters tests of the IPENPM and the over-charge/discharge protection tests at the fixed-illumination of 200 lux. Section IV reports the application of powering the IoT gas sensor node to measure CO_2 concentration at 200 lux indoor lighting for automatic building air quality control. Section V concludes this paper.

II. IPEHPM for IoT-Based Gas Sensing

A. Power Requirement

The nondispersive infrared CO_2 sensor developed by GSS has been reported to have 50 times lower power consumption than its counterparts [12]. It integrates a fast response gas sensor and signal conditioning circuits to measure CO_2 concentration from 0 to 5000 ppm with +/−50 ppm accuracy.

TABLE I
Power Requirements for an IoT-Based CO_2 Sensor Node

Supply voltage	Peak current	Sleep mode Current
3.5~5.5 V	30 mA for 150 ms	4 μA

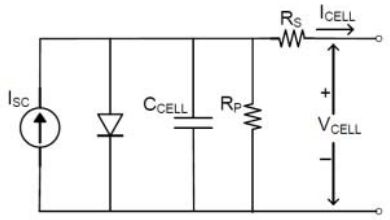

Fig. 1. Circuit model of a single PV cell which shows the PV cell as a current source and the open-circuit voltage is restricted by the diode.

The wireless sensor node is implemented using the Moteino development platform (LowPowerLab LLC, Canton, MI, USA) including a low-power 868 MHz ISM band RF transceiver of Hope RF RFM69HW which consumes 16 mA at 4.8 kb/s in transmission mode and a microcontroller of ATMega328 which consumes 6.5 mA in active mode and 4 μA in sleep mode. In sleep mode the microcontroller works in power-save mode, where the asynchronous timer runs continuously to maintain a timer base while the rest of the device is sleeping. The timer will produce an interrupt which wakes-up the system.

The total power requirements of the GSS COZIR CO_2 gas sensor [12] are listed in Table I.

The power consumption specified for the gas sensor is 3.0 mW at 3.3 V supply for two measurements per second in continuous measuring mode. If the gas sensor is utilized every 150 s, the required average current of the gas sensor can be estimated as (3.0 mW/3.3 V $\times$ 1/2 s + 150 s $\times$ 4 μA)/150 s = 11 μA.

Assume that the IoT node works for 100 ms for sensor control and data transmission (to transmit five ASCII messages for a gas measurement), the required average current is (16 + 6.5) mA $\times$ 100 ms/150 s = 15 μA. Therefore, to power an IoT-based gas sensor node, a total average current of 26 μA is required, corresponding to 91 μW power consumption at 3.5 V supply.

B. High Efficiency PV Energy Harvesting Module

A PV panel can hardly act as a power supply alone since its output power varies with illumination conditions. The equivalent circuit diagram of a PV cell is shown in Fig. 1, where I_{sc} represents the photon current which is proportional to intensity of incoming light (illumination) and the area of the cell, and I_0 presents the leakage of the electrons and carrier recombination. R_p denotes the shunt resistance representing the loss incurred by conductors, and the R_s represents the loss of non-conductors. The output current of the PV cell is expressed in the formula

$$I_{\text{cell}} = I_{\text{sc}} - I_0\left[\exp\left(\frac{V_{\text{cell}} + R_s I_{\text{cell}}}{\frac{KT}{q}}\right) - 1\right] - \frac{V_{\text{cell}} + R_s I_{\text{cell}}}{R_p}. \quad (1)$$

Since R_p is large and R_s is small, the output current of the PV cell is almost a constant of I_{sc} determined by the illumination. The output voltage of the PV cell V_{cell} depends on the load of the PV panel. Formula (1) is not a practical formula so its graphic form is commonly used.

A high-efficiency PV energy harvesting module has been developed for efficient conversion of indoor light. These are typically artificial sources, such as incandescent and fluorescent for current markets, and LED for future/emerging indoor lighting deployment [13]. The PV energy harvesting module has an area of 50 mm $\times$ 20 mm. The open-circuit voltage range of the PV energy harvesting module is $4.0 - 4.9$ V when light intensity changes from 10–1000 lux. At the indoor low illumination condition of 200 lux, the open-circuit voltage of the PV energy harvesting module is 4.6 V (larger than the required 3.5 V) and the short-circuit current is 45 μA (larger than the required 26 μA). Therefore, it is apparent that PV energy harvesting module can provide enough energy for IoT-based building ventilation applications at illumination conditions down to 200 lux.

C. Energy Storage Component

The harvested energy can be stored in a rechargeable Lithium battery or a supercapacitor. Storage capacity, self-discharge and lifetime are three key parameters to be considered in storage selection. For powering low-power IoT nodes, the required capacity can be achieved by both storage components, while longer lifetimes make supercapacitors the better storage selection for fit and forget IoT applications, although it is believed that the high self-discharge current of the supercapacitor limits the wide use of the supercapacitor in IoT devices [14].

The μA level self-discharge current of the supercapacitor can be ignored in outdoor PV energy harvesting applications, where current output is significantly higher, such as in mAs, while for indoor applications the current output can be as low as 10 s of μA so self-discharge current should not be ignored. The self-discharge current of the supercapacitor changes with time and it is reported as being large in the first hours after charging [15], while the self-discharge specification of the supercapacitor adopted in this design (VinaTech 5.4 V 0.5 F) is 2.0 μA after 72 h post charging. In IoT applications, the storage supercapacitor is repeatedly charged and discharged during every measurement period which is highly unlikely to be longer than 72 h, therefore the actual value of the supercapacitor self-discharge which is an essential technical parameter for low-power applications should be evaluated. By now this value is missing since the charge redistribution issue [15] raised by the effects of double-layer capacitance with electrolyte in the supercapacitor makes the leakage test a challenge.

D. Power Management Scheme

Power management is required to maximize use the harvested energy from PV energy harvesting since the harvested ambient energy is usually very weak (20+% PV energy converting efficiency in this high efficient PV panel), while maximum power output is not required in a general power supply, where input power is supposed to be unlimited. It is also required protecting the storage components from overcharge (resulting in degraded performance, such as increased equivalent series resistance, or overheating) and over-discharge to prolong the lifetime of energy storage components [16].

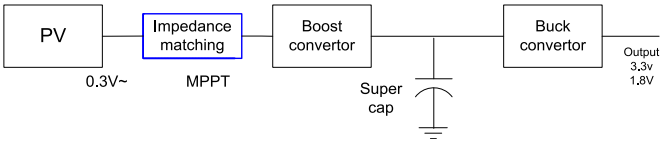

Fig. 2. Block diagram of a typical commercially available power management chip for PV energy harvesting.

The block diagram of a typical commercially available power management chip is shown in Fig. 2, where a voltage boost stage is required since the open-circuit voltage of a PV cell (which is the highest output voltage of the PV cell) is limited by the forward voltage drop of the diode of the PV cell typically around 0.7 V, while a typical commercially available IoT node chip requires 3.3 V or 1.8 V supply. MPPT circuits are included since the output impedance of the PV cell changes from a few kΩ to tens of KΩ depending on the illumination conditions while the input impedance of the boost convertor stays constant with illumination. Therefore, the impedance between the PV cell and the voltage booster has to be matched in order to extract maximum energy from the PV energy harvester. The storage voltage might be higher than 3.3 V due to the tradeoff between storage capacity ($CV^2/2$) and self-discharge, since it is reported that the self-discharge of a supercapacitor is significantly higher when the terminal voltage is higher than 85% of the voltage rating [17]. Another power regulator might be required to boost/buck convert the storage voltage to the required supply voltage. A challenge comes to this project is that the adopted 10 cm^2 PV panel working at 200 lux could not drive any commercially available power management chip (the energy harvested is lower than that consumed by the power management chip). Therefore, power management functions should be simplified to save power.

Unlike the general PV energy harvesting applications, where maximum harvesting and storing energy is the highest priority, the PV energy harvesting used in this project is to continuously power the IoT node which has a rated power consumption. The *I–V* and the *P–V* curves of the adopted PV panel shown in Fig. 3 demonstrate that when illumination condition is getting better, the output power of the PV increases. Therefore, as long as the energy harvested at 200 lux is high enough to drive the senor node, MPPT is not required for a better illumination case since the output power at a better illumination condition is definitely higher than that at 200 lux for same operating voltage. The conclusion of the power management requirement for powering IoT node is to ensure that PV works in the high power region at 200 lux to get rid of MPPT (which tracks the maximum output power for different illumination conditions) for power saving. In fact, MPPT is a power hungry block [18], [19] since it requires

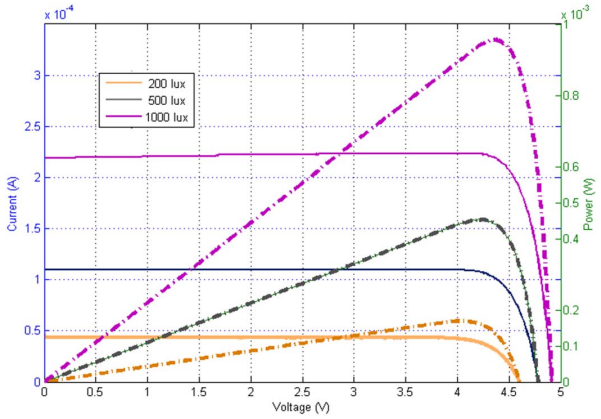

Fig. 3. *I–V* (solid line) and the *P–V* curves (dashed line) of the PV energy harvesting module at different indoor illumination conditions.

measurement of the open-circuit voltage of the PV energy harvester, or an extra photo diode, which is a miniaturized on-chip PV energy harvester acting as the light sensor [20] or complicated signal processing circuits, such as a successive approximate register or a digital signal processor to track the maximum power point. The impedance matching needs to be implemented for example by a voltage controlled oscillator to continuously tune the switching frequency of a capacitor to adjust the load impedance ($R = 1/(f \times C)$) of the PV energy harvester. As a result, MPPT power consumption reported in [21] is 140 μW, which is relatively large when compared to the 160 μW maximum power produced by the adopted PV at 200 lux.

With the high open-circuit voltage of the PV energy harvesting module employed in this paper, the boost convertor shown in Fig. 3 is not necessary for powering the IoT-based sensor node, so a simple charger without commonly adopted MPPT [4], [18], [19], [22]–[24] has been used as the power management in this design providing a power efficient solution.

1) Storing Energy in Supercapacitor With Simple Charger: A battery charger, LTC4071 from linear technology with power management functions of over-charge and over-discharge protections, has been employed for power management in the IPEHPM. The simplified block diagram of the IPEHPM is shown in the top of Fig. 4. The PV energy harvester is connected to R_{in}, the storage supercapacitor is connected to "BAT" pin, while the load of the IPEHPM will be connected to V_{cc}. At the beginning, when the supercapacitor voltage is lower than the over-discharge protection voltage transistor MP_1 is off, so the IPEHPM is inactive. When the voltage of the supercapacitor is charged higher than 3.6 V through the charge path of R_{in} and the diode, MP_1 is switched on to activate the IPEHPM enabling to output a high power pulse from storage. When the voltage of the supercapacitor is charged as high as the over-charge protection voltage (4.0 − 4.2 V selectable), the charge current will be shunted through MP_2 so that the voltage of the supercapacitor will not increase any further.

A simplified top-level IPEHPM diagram is shown in the bottom of Fig. 4, which demonstrates that in the simple charger

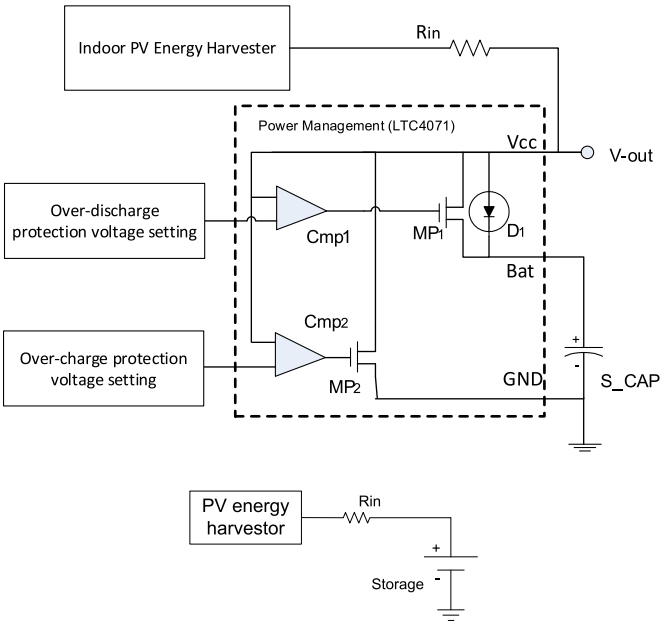

Fig. 4. Block diagram of the top: IPEHPM with the battery charger from linear technology and bottom: the simplified top-level circuit of IPEHPM.

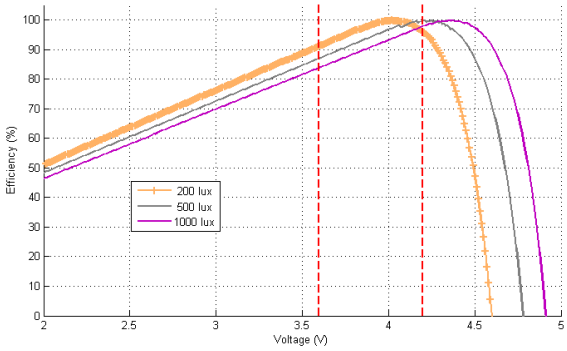

Fig. 5. Normalized output power efficiency of PV energy harvesting module versus operating voltage at different illumination conditions.

scheme the output voltage of the PV energy harvesting module has been directly set as the storage voltage.

2) Storage Efficiency Analysis: The normalized output power efficiency of the PV energy harvesting module is shown in Fig. 4, where maximum output power for each illumination condition is treated as 100%, demonstrating that the operating voltage at the maximum output power point changes with the illumination conditions, so MPPT seems necessary to track the changing illumination condition in real-time. However, as shown in Fig. 5, if operating voltage of the PV energy harvesting module is set in a defined region, such as 3.6–4.2 V by the supercapacitor together with the power management chip of LTC4071 as shown in Fig. 4, higher than 80% efficiency can be directly obtained for all indoor illumination conditions (200 to 1000 lux) without MPPT. Therefore, after the IPEHPM is active (>3.6 V output), and if the harvested energy is higher than that of application required, MPPT will not be required since the voltage of the storage will keep increasing until over-charge protection voltage (maximum of 4.2 V) is reached. In this way, the PV energy harvesting

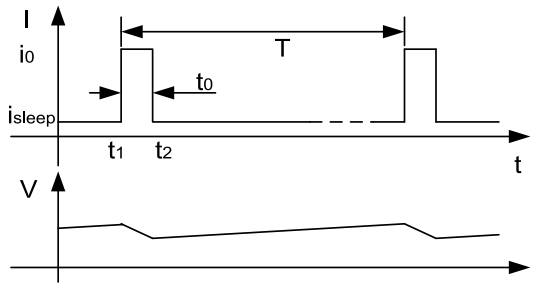

Fig. 6. Current profile and supply voltage curve when an IoT node is powered by the IPEHPM. In a measurement period of T, there is a large current pulse i_0 within t_0 (active node) and a tiny current i_{sleep} (sleep mode) during the long sleep period.

module will always work in the voltage range of 3.6–4.2 V for high power output efficiency at indoor illumination conditions.

E. Powering IoT Node by the IPEHPM

Unlike the conventional power supply whose power is irrelative to illuminations or in the case of PV energy harvesting acting as an auxiliary power source with MPPT focusing on maxim using harvested power rather than how much the maximized power is, the developed IPEHPM should be linked the IoT power requirements to the PV panel size and illuminate condition so that the harvested PV energy can be utmost used.

An energy-based powering model is established to directly evaluate whether IPEHPM is capable of powering the IoT node at a specific illumination condition. The required power consumption for a specific IoT application can be converted into the current profile as shown in the top of the Fig. 6, where i_0 and t_0 denote the current and time duration in active/measurement mode, i_{sleep} denotes the current in the sleep mode and T denotes the measurement period. The voltage output of the IPEHPM is shown in the bottom of the Fig. 6, where V_{t1} (the voltage at t_1) is higher than V_{t2} (the voltage at t_2). To keep the IoT node working continuously, the start voltage of the next measurement period should not be lower than V_{t1}.

According to the energy flow model [25], the total energy harvested $\int_{\tau=0}^{t} P_{\text{scv}} d\tau$ should be greater than the energy required $\varepsilon_{\text{DEV}}(t) = \int_{\tau=0}^{t} P_{\text{scv}} d\tau$

$$\varepsilon_{\text{BUF}}^{t=0} + \int_{\tau=0}^{t} P_{\text{scv}} d\tau \geq \int_{\tau=0}^{t} P_{\text{scv}} d\tau = \varepsilon_{\text{DEV}}(t) \tag{2}$$

where $\varepsilon_{\text{BUF}}^{t=0}$ denotes the energy initially stored.

In the IPEHPM, the energy stored in the supercapacitor in sleep mode is $(1/2)\text{CV}_{t1}^2 - (1/2)\text{CV}_{t2}^2$, and the energy consumed in active mode is $(i_0 - i_{e\_c}) \int_{t1}^{t2} V_\tau d\tau$ when equivalent active current is treated as $(i_0 - i_{e\_c})$ so no energy is stored in active period, where the effective charge current, which is the charge current of the PV energy harvester (I_{pv}) minus both the in-circuit self-discharge current of the supercapacitor (I_{leak}) and the quiescent current of the power management chip (I_q) as shown in Fig. 7.

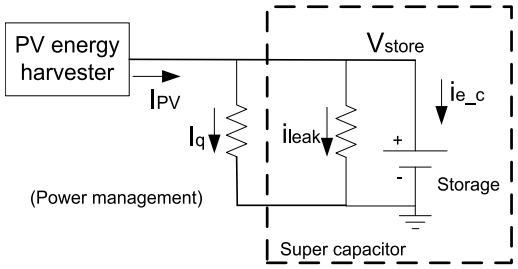

Fig. 7. Circuit diagram shown current relationship in the power module.

According to (2), to keep the IoT node running continuously, it holds

$$\frac{1}{2}\text{CV}_{t1}^2 - \frac{1}{2}\text{CV}_{t2}^2 \geq \left(i_0 - i_{e\_c}\right) \int_{t1}^{t2} V_\tau d\tau \tag{3}$$

where C denotes the capacitance of the storage and V denotes the voltage of the storage. Considering that the discharge current in the active mode is not a constant (the load current minus the effective charge current) at a given illumination, the output voltage drop of the IPEHPM in the active period caused by discharging the supercapacitor should be nonlinear. It holds in the low illumination conditions, where PV currents are lower than the active discharge current

$$\int_{t1}^{t2} V_\tau d\tau < \frac{1}{2}(V_{t2} + V_{t1})(t_2 - t_1) = \frac{1}{2}(V_{t2} + V_{t1})t_0. \tag{4}$$

Therefore, if

$$\frac{1}{2}\text{CV}_{t1}^2 - \frac{1}{2}\text{CV}_{t2}^2 \geq \left(i_0 - i_{e_c}\right)\frac{1}{2}(V_{t2} + V_{t1})t_0 \tag{5}$$

works then (3) will definitely work, since $(1/2)\text{CV}_{t1}^2 - (1/2)\text{CV}_{t2}^2 \geq (i_0 - i_{e_c})(1/2)(V_{t2} + V_{t1})t_0 > (i_0 - i_{e\_c}) \int_{t1}^{t2} V_\tau d\tau$.

Formula (5) becomes

$$\frac{1}{2}C\left(V_{t1}^2 - V_{t2}^2\right) \geq \frac{1}{2}(V_{t1} + V_{t2})\left(i_0 - i_{e\_c}\right)t_0. \tag{6}$$

After cancelling down $(1/2)(V_{t1} + V_{t2})$ from both sides, (6) becomes

$$C(V_{t1} - V_{t2}) \geq \left(i_0 - i_{e_c}\right)t_0. \tag{7}$$

The term of $C(V_{t1} - V_{t2})$ on the left side of (7) is the total charge of the supercapacitor during $(t_1 + T) - t_2 = T - t_0$, and therefore in this period the supercapacitor holds

$$C(V_{t1} - V_{t2}) = \left(i_{e\_c} - i_{\text{sleep}}\right)(T - t_0). \tag{8}$$

Formula (6) finally becomes

$$i_{e\_c} T \geq i_0 t_0 + i_{\text{sleep}}(T - t_0). \tag{9}$$

Formula (9) represents a charge/discharge model for the energy storage supercapacitor, showing that to power an IoT node working continuously, the total charge the storage supercapacitor receives from the PV energy harvester $i_{e-c} \times T$ should be no less than the total discharge of the storage supercapacitor by the IoT node in a measurement period as $I_0 \times t_0 + I_{\text{sleep}} \times (T - t_0)$, guaranteeing that the output voltage of the storage supercapacitor will not decrease over the next measurement when (9) holds.

Fig. 8. 50 mm × 20 mm × 15 mm IPENPM. Top: PV energy harvesting module side of the IPEHPM. Bottom: electronic components side of IPEHPM.

The simplified IPEHPM power model shown in (9) links all application parameters, such as illumination condition (i_{e_c}), measurement period (T), current pulse amplitude (i_0) and duration (t_0), and the sleep mode current (i_{sleep}). Therefore, the powering capability of the IPEHPM for a specific IoT node can be directly evaluated using (9). Since the total discharge is a known value for a specific application, the lowest illumination condition for an IoT application can be determined by calculating i_{e-c} using (10) and then using i_{e-c} to determine a suitable illumination condition

$$i_{e\_c} > \frac{i_0 t_0 + i_{\text{sleep}}(T - t_0)}{T}. \tag{10}$$

Note that the right part of (10) is the average load current of the IoT node. Therefore, (10) can be easily explained as the effective charge current of the IPEHPM should not be less than the average load current of the IoT node.

Similarly, for a specific illumination condition, the minimum available measurement period can be calculated via (9) as well

$$T > \frac{(i_0 - i_{\text{sleep}})t_0}{i_{e\_c} - i_{\text{sleep}}}. \tag{11}$$

In practice, if the output voltage of the IPEHPM reaches the overvoltage protection voltage for a while, there is a possibility of either shortening the measurement period to acquire more measurement data or lowering the illumination condition to ease the lighting restrictions.

III. Performance Tests and Functionality Validations

The IPEHPM has been designed and fabricated as shown in Fig. 8. The schematic of the IPEHPM has already been shown in Fig. 3. A low voltage drop Schottky diode has been added between the PV energy harvester output and R_{in} to protect the PV energy harvester being charged by the storage when illumination conditions are poor.

All electronic components are mounted on the bottom layer of the PCB. The PV energy harvesting module, which has the same dimension of the PCB, has been soldered on the top layer of the PCB. The fabricated IPEHPM has a dimension of 50 mm × 20 mm × 15 mm.

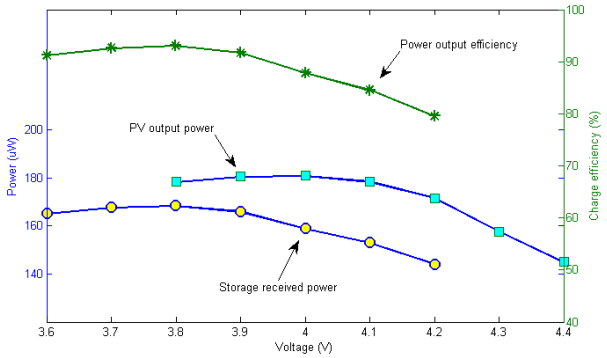

Fig. 9. Output power of the PV energy harvesting module (blue), storage received power (purple), and the storage efficiency (green curve).

A. Storage Efficiency

Storage efficiency of the IPEHPM has been examined using the designed PCB by replacing the energy storage supercapacitor with a Keithley source-meter acting as a voltage source so that the charge current flowing into the storage can be measured at different operating voltages when the PV energy harvester is illuminated at 200 lux. Varying the voltage of the Keithley source-meter from 3.6 to 4.2 V with a 0.1 V voltage step, the current flowing into the Keithley, together with the PV output current and the output voltage has been recorded at the same time.

Fig. 9 shows that the maximum output power of the PV energy harvesting module (the blue curve marked with "□") is 180.95 μW when the output voltage of the PV energy harvester is at 4.0 V, while the maximum power the storage received (the blue curve marked with "○") is at the voltage of 3.8 V. The 0.2 V difference is caused by the voltage drop measured across the protection Schottky diode.

Power output efficiency of the power module has been calculated by dividing the storage received power by the maximum PV energy harvesting module output power, as shown in Fig. 6 (the green curve marked with "*"). The achieved maximum storage efficiency is 93.1% at the storage voltage of 3.8 V while the minimum one is 79.6% at that of 4.2 V. The average storage efficiency is 88.7% for the tested storage voltage range of 3.6–4.2 V, demonstrating that the IPEHPM has achieved high storage efficiency at 200 lux.

Since the additional Schottky diode introduces 0.2 V voltage shift between the output voltage of the IPEHPM and the PV energy harvester output voltage, the average efficiency of the IPEHPM depends on the over-charge protection voltage setting. The average efficiency reaches 91.3% for 4.0 V over-charge protection setting and 90.2% for 4.1 V over-charge protection setting of the IPEHPM.

The *I–V* curves at different illuminations shown in Fig. 3 demonstrate that the *I–V* curve at the higher illumination conditions is a magnified curve of the lower illumination one in both I- and V-axes, therefore the output power at the higher illumination is always larger than that at the lower illumination. As a result, as long as the power output at the worst illumination condition (200 lux in this design) meet the application requirements, it will have no problem for better illumination conditions.

TABLE II
EFFECTIVE CHARGE CURRENT (I_{ef}) AT DIFFERENT ILLUMINATION CONDITIONS

Illumination (lux)	100	200	300	400	500	1000
I_{e_c} (μA)	18.4	38.6	61.2	82.0	99.5	212.1

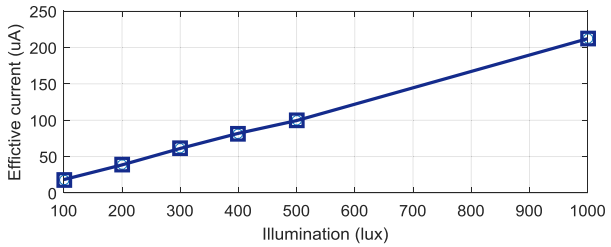

Fig. 10. Effective charge current versus illumination condition.

The key point of using PV energy harvesting under indoor illumination conditions without MPPT is to find a way to set PV energy harvester operating voltage in high efficiency range for the worst illumination conditions. This issue has been solved in the IPEHPM by using a charger which sets the PV energy harvester operating voltage as 3.8–(4.2–4.4) V. At 200 lux a 2.6% storage efficiency increase can be achieved by sacrificing 9.3% storage capacity when over-charge protection voltage is set as 4.0 V in IPEHPM.

B. PV Energy Harvesting Power Module Parameter Tests

1) Effective Charge Current: As mentioned previously, the charge efficiency changes with operating points and the in-circuit self-discharge current of the supercapacitor is suspected to be larger than the steady self-discharge current, making the performance of the IPEHPM difficult to evaluate based on the *I–V* curve of the PV. However, when considering that a full charge-discharge circle from 3.6–4.2–3.6 V with the load pattern shown in Fig. 5, the parameter of the effective charge current (i_{e_c}) of the IPEHPM at different illumination conditions has been measured. The results are listed in Table II and shown in Fig. 10.

2) Resistance and Maximum Output Current: The resistive impedance of the IPEHPM has been measured by recording the offset voltage changes when two different discharge currents supplied by a Keithley source-meter are swapped. The measured resistance is 5.5+/−1.0 Ω. Therefore, outputting a high current from the IPEHPM can result in a relatively high output voltage drop (mainly dropped across MP_1 in the power management chip shown in Fig. 2 due to its on-resistance). For low-power applications, such as the 20 mA current pulse, the maximum output voltage drop in active mode is less than 130 mV which is insignificant (4% of the supply voltage of 3.3 V).

The output current of the IPEHPM is specified by the absolute maximum discharge current. The maximum pulse current has been tested when the IPEHPM is active with an output voltage of 4.2 V. The pulse duration has been defined as the output current dropping by 5% of its value.

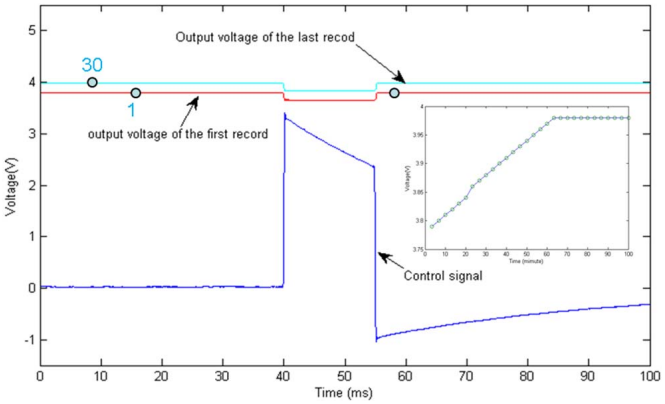

Fig. 11. Recorded voltage signal change between active and sleep modes with the mode control signal (blue). The voltage drop in active mode (control = high) shows the effect of the internal resistance. The inset figure shows the voltage of the IPEHPM measured in the sleep mode for 30 measurement periods (data points of 1, 2, and 30 have been labeled in the main figure).

Since the maximum resistive impedance of the power module is 6.5 Ω and the lowest output voltage is 3.5 V for the CO_2 sensor, the available maximum output current is calculated as (4.2–3.5 V)/6.5 Ω = 107 mA. So the test pulse current for the power module was set as 100 mA for the maximum pulse discharge current test. The duration of the 100 mA current pulse has been measured by setting the variable load resistor to 42 Ω. It takes 645 ms for the output voltage to drop by 5%. Therefore, the 100 mA pulse duration is at least 600 ms, significantly exceeding the application requirements for building ventilation specified in Section II-A.

C. Functionality Validation at 200 lux

The functions of over-charge and over-discharge of the IPEHPM have been validated by two switched load resistors to mimic a 30 mA active pulse current and 4 μA sleep mode current of an IoT node (125 Ω for active mode and 1 MΩ for sleep mode). The switch control signal (15 ms pulse every 200 s) has been generated by a pattern generator. The experimental data has been recorded by an Agilent DSA90000 oscilloscope working in the segmented memory mode triggered by the switching control signal. The over-charge protection voltage of the IPEHPM is set to 4.0 V and the storage has been initially set as 3.8 V so that an increasing output voltage can be easily observed if the harvested energy is larger than the demanded energy.

Fig. 11 shows two recorded output voltage signals (red and cyan) together with the IoT working mode control signal (blue, high level = active mode, low level = sleep mode) from 30 measurement periods. The voltage of the first recorded signal (red curve) is 3.79 V in sleep mode and 3.65 V in active mode, demonstrating a ∼30 mA output current and a 140 mV voltage drop produced by the internal resistance of the power module. Similarly, the voltage in sleep mode and that in active mode can be seen as the output voltage of the last measurement (cyan curve). The output voltage of the IPEHPM measured in sleep mode is shown inset within Fig. 11, where

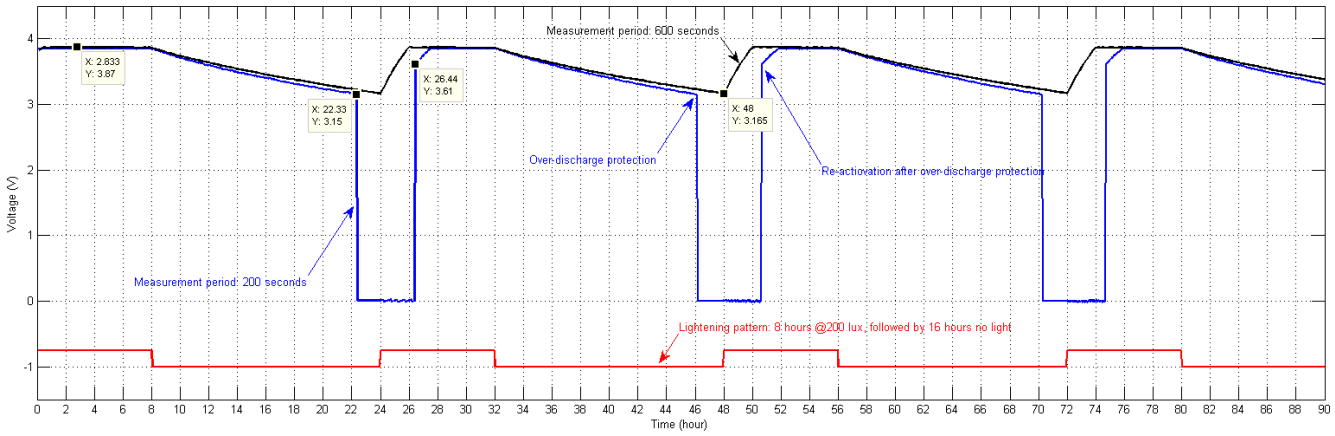

Fig. 12. Output voltage of IPEHPM measured in active mode. Blue trace is for IoT node measuring every 200 s and the black curve is for 600 s case. The daily repeated lighting pattern (red trace) is 8 h at 200 lux, then followed by 16 h without light. The over-discharge protection (0 V output voltage of IPEHPM in active mode) and IPEHPM load reconnect (3.6 V output voltage) can be observed in the blue curve.

the data points of 1 and 30 have been labeled in the main figure.

An almost linear output voltage increase and the over-charge protection (flat part of the curve) can be observed in the sleep mode voltage curve.

A 200 lux illumination experiment has been carried out over four days to examine the over-discharge protection and reactivation after over-discharge protection. It starts with a fully charged IPEHPM working at 200 lux for 8 h, followed by 16 h without light, and then repeats the lighting pattern for several days. The output voltage signal recorded in active mode (blue trace) together with the lighting pattern (red trace) is shown in Fig. 12. Results show that in the first 8 h, the output voltage is a constant, and then when the light is off the output voltage decreases. After 22 h the output voltage dropped to 0 V due to over-discharge protection. At 24 h the illumination returned to charge the storage, and after about 2 h the storage was charged to 3.61 V which enabled the IPEHPM become active. Then the output voltage increased within the next 2 h, and maintained at 3.86 V due to the overcharge protection until the illumination is off. Repeating experiment for another two days, the power module has worked properly with over-charge and over-discharge protections, and reactivation.

By adjusting the measurement period from 200 to 600 s based on the calculation of the minimum available measurement period using (10) and repeating the experiment, the black curve shown in Fig. 12 demonstrated a continuous decreasing output voltage when there is no light and then a continuous output increasing until the over-charge protection voltage is reached when light is on. No over-discharge protection happened in this case.

IV. IoT Experiments With the CO_2 Gas Sensor

A. Powering Requirements

The current profile of the IoT-based CO_2 gas sensor in polling mode (sensor reports readings only when requested) has been measured as shown in Fig. 13 with a bench power supply, where the first pulse is the wake-up current of the gas sensor, followed by two current pulses for sensor excitation and data reading, and then the last pulse for RF transmission. Note that all current pulses are within the IPEHPM specifications of 100 mA at 600 ms. The required total discharge of the storage supercapacitor in IPEHPM module for one measurement in every 150 s has been calculated as 4.24 mC.

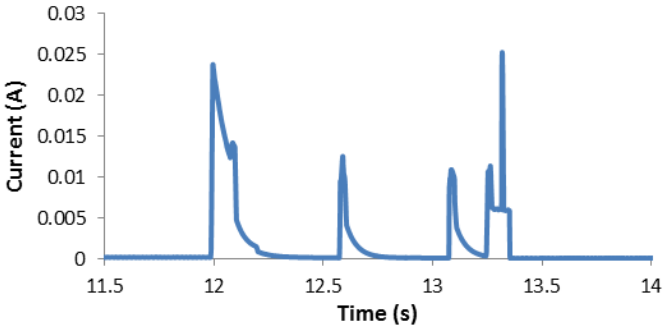

Fig. 13. Measured current profile of GSS gas sensor in low-power polling mode for one CO_2 measurement (pulses from left to right: wake-up, sensor excitation, data reading, and the data transmission).

B. Experiment Set-Up and Measurement Results

Setting the measurement period as 150 s, the CO_2 sensor, together with the IoT node circuits (MCU and wireless communication, refer to Section II-A), was powered by the IPEHPM at the fixed illumination condition of 200 lux provided by a SCHOTT LED light source (KL 1600, 55122 Mainz, Germany) outside the experiment chamber as shown in the top of Fig. 14. Another CO_2 sensor which is directly powered from an USB cable has been placed inside the experiment chamber to concurrently measure CO_2 concentration as the reference measurement. The RF output power of the sensor node has been set as -1 dBm.

The CO_2 concentration measurement data has been transmitted to the gateway node which is connected to the host PC which has been placed 10 m away for data recording and the output voltage of the IPEHPM has been recorded

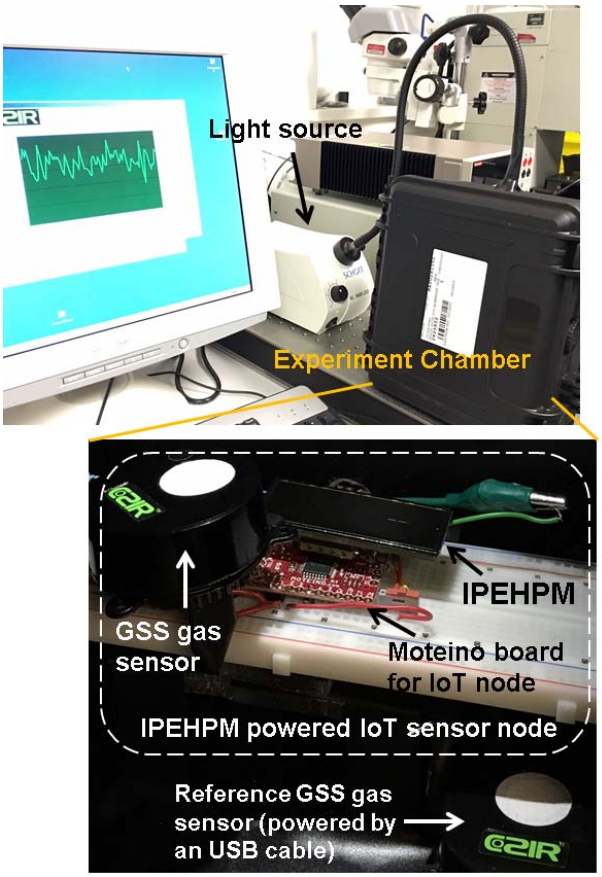

Fig. 14. Experiment set-up. Top: experiment chamber, light source, and GSS GUI. Bottom: inside the experiment chamber. The dashed line block shows the IoT sensor node powered by IPEHPM (GSS gas sensor, IPEHPM, and Moteino including MCU plus wireless circuits). A reference GSS gas sensor powered by an USB cable is shown in the bottom.

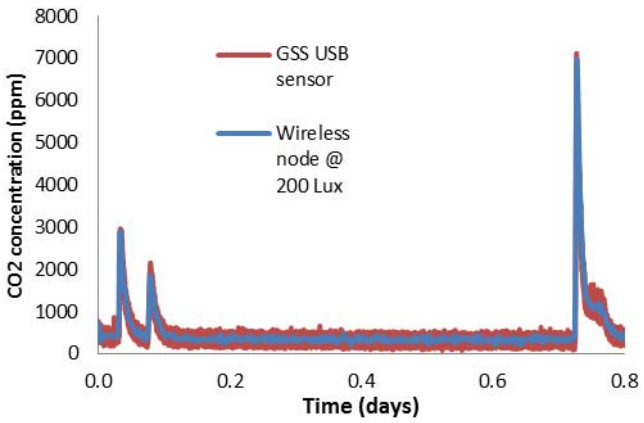

Fig. 15. Measured CO_2 concentration level traces from the IPEHPM powered IoT-based GSS sensor (blue trace) and the USB-powered one (red trace).

by a Keithley multimeter (DMM7510). The CO_2 level of the USB powered gas sensor was also recorded. The experiment was continuously running for 20 h in a controlled environment that had high levels of CO_2 introduced three times.

The measured output voltage of the IPEHPM over the first 0.14 days is shown in Fig. 16, which shows a rising output voltage at the beginning and then a constant voltage

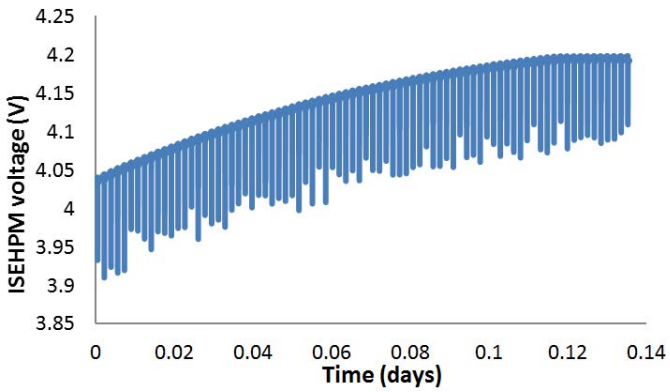

Fig. 16. Measured output voltage of the IPEHPM at the first 0.14 days. The spikes are the voltage output in active mode. The rising and then flat envelope demonstrated that the harvested energy is higher than the application demands.

TABLE III
ENERGY SUMMARY OF THE IPEHPM FOR POWERING CO_2 CONCENTRATION MEASUREMENTS AT 200 lux (ENERGY HARVESTED, STORED, AND CONSUMED IN μW)

Maximum output power of the PV energy harvester	45.0×4.0 = 180.0
Actual PV energy harvester output power (average)	88.7%×180 = 159.7
Available power from IPEHPM	38.6×3.6 = 139.0 (min) 38.6×4.2=162.1 (max) 150.5 (average)
Power consumed by the IoT node	28.3×4.2 = 118.9 (max)

(over-charge protection) at 0.12 days when sleep mode output voltage is 4.2 V, indicating that the energy harvested was higher than the amount the sensor demanded. The ∼120 mV voltage spikes between sleep mode and active mode are caused by the internal resistance when 20 mA current is supplied by the IPEHPM for RF transmission.

The fact that the CO_2 sensor with IoT node can be powered by the IPEHPM is discussed hereafter. As shown in Table III, the effective charge current of the IPEHPM is 38.6 μA at 200 lux, so the total charge the PV energy harvester provided is 5640 μC in the whole measurement period of 150 s, which is larger than the demanded discharge of 4240 μC in a measurement period. As the result, the output voltage of the IPEHPM increased and then maintained the same as the over-charge protection voltage.

Table III lists the energy harvested by the PV energy harvester module at 200 lux, stored in the IPEHPM and consumed by the IoT node during the CO_2 concentration measurement experiment, which demonstrated that the power consumed by the IoT node is less than the power available from the IPEHPM at 200 lux. Since the output power of the PV energy harvesting module is getting larger when illumination condition improved, the newly developed IPEHPM is able to power the IoT-based GSS gas sensor to measure CO_2 concentration every 150 s for building ventilation at the illumination down to 200 lux.

PV energy harvesting approaches for powering applications have been compared to this paper in Table IV in terms of the adoption of functional blocks of dc–dc convertor, MPPT

TABLE IV
FUNCTIONAL BLOCKS INCLUDED AND THE ILLUMINATION RESTRICTION OF POWERING APPLICATIONS USING PV ENERGY HARVESTING

	DC-DC convertor	MPPT	Illumination restriction
[18]	Yes	Yes	No
[26]	Yes	No	Yes
[21]	No	Yes	No
This work	No	No	No

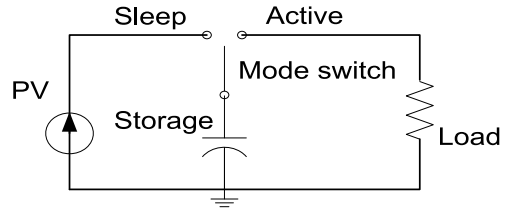

Fig. 17. Top-level circuit model of the IPEHPM with the load of an IoT node.

and illumination restrictions. Compared to other powering applications, such as powering indoor low-power system with MPPT [14], using assumption of fixed indoor illumination to exempt MTTP [26] and the "storage-less and converter-less" strategy with MPPT for powering the IoT [21], the simple charger power management scheme employed in the newly designed IPEHPM provides a dc–dc convertor-free and MPPT-free solution, enabling powering IoT nodes using PV energy harvesting at all indoor illumination conditions with the minimum power consumption.

C. Discussion

1) PV Powering Model: It is worth noting that the output voltage drop in the nonlighting period shown in Fig. 12 (refer to time from 8 to 22 h) is slightly nonlinear. This is because in the top-level circuit model of the IoT node powered by the IPEHPM, which is shown in Fig. 17, the energy storage in sleep mode can be more likely described as the supercapacitor charging from a constant current while the energy consuming in active mode is described as the supercapacitor discharge in an *RC* circuit (*R* represents the load resistance in active mode, *C* represents the capacitance of the supercapacitor), since the charge current in sleep mode is mainly determined by the PV energy harvester which outputs a constant current at a specific illumination but the discharge current in active mode reduces with the decreasing supercapacitor voltage in the discharging process.

The output voltage of the supercapacitor (V_1) changing with time (t) in the discharge period (active mode) is expressed as

$$V_1 = V_0 \exp\left(-\frac{t}{RC}\right) \tag{12}$$

where V_0 is the initial voltage of the supercapacitor.

As shown in Fig. 6, discharge current in the active mode is supposed to be a constant of i_0 which can be calculated as V_0/R. Therefore, under this constant current discharge assumption the output voltage of the supercapacitor (V_2) can be expressed as

$$V_2 = V_0 - \frac{i_0}{C}t = V_0\left(1 - \frac{t}{RC}\right). \tag{13}$$

According to Taylor expansion, the exponential term in (12) can be expressed as

$$\exp\left(-\frac{t}{RC}\right) = \sum_{n=0}^{\infty} \frac{\left(-\frac{t}{RC}\right)^n}{n!} = 1 - \frac{t}{RC} + \frac{\left(\frac{t}{RC}\right)^2}{2} - \frac{\left(\frac{t}{RC}\right)^3}{2\times 3} + \cdots \tag{14}$$

Since

$$\frac{d}{dt}\left[\frac{\left(\frac{t}{RC}\right)^2}{2} - \frac{\left(\frac{t}{RC}\right)^3}{2\times 3} + \cdots\right] = \frac{t}{RC} - \frac{\left(\frac{t}{RC}\right)^2}{2} + \cdots = 1 - \exp\left(-\frac{t}{RC}\right) \geq 0 \tag{15}$$

and

$$\left.\frac{\left(\frac{t}{RC}\right)^2}{2} - \frac{\left(\frac{t}{RC}\right)^3}{2\times 3} + \cdots\right|_{t=0} = 0. \tag{16}$$

Therefore,

$$\frac{\left(\frac{t}{RC}\right)^2}{2} - \frac{\left(\frac{t}{RC}\right)^3}{2\times 3} + \cdots \geq 0. \tag{17}$$

The relationship of the voltage drop in active mode in an exponential way (V_1) and in a constant current linear way (V_2) can be derived from (12) and (14) as

$$\begin{aligned} V_1 &= V_0 \sum_{n=0}^{\infty} \frac{\left(-\frac{t}{RC}\right)^n}{n!} \\ &= V_0\left(1 - \frac{1}{RC}t + \sum_{n=2}^{\infty} \frac{\left(-\frac{t}{RC}\right)^n}{n!}\right) \\ &\geq V_0\left(1 - \frac{t}{RC}\right) \\ &= V_2. \end{aligned} \tag{18}$$

Formula (18) shows that the actual output voltage drop of the IPEHPM in the discharge process is not larger than that predicted when using a constant discharge current. Therefore, (10) and (11) provide a simplified solution which presents the worst case situation of using the IPEHPM.

2) Dynamic Leakage Current of the Supercapacitor: The measured maximum dynamic leakage current of the IPEHPM implemented for each charge-discharge period in the IoT experiment is 2.4 μA. Considering that the maximum quiescent current of the power management chip is less than 0.5 μA, the in-circuit dynamic leakage current of the supercapacitor is around 2.0 μA in this experiment, which is almost the same as the leakage current specified after 72 h post charging. The explanation of this test result is that in this experiment, the percentage of charge and discharge to the full storage capacity is relatively low. The total charge in a measurement period is 45 μA $\times$ 150 s = 6.75 mC which is about 0.3% of the full storage capacity of the supercapacitor as 0.5 F $\times$ 4.2 V = 2.1 C, while the total discharge is less than 4.5 mC which is about

0.2% of the full storage capacity. Also the highest working voltage of 4.2 V is 77% of the rating voltage of the supercapacitor, which is low than the 85% reported for high leakage [11]. Therefore, the supercapacitor almost stays in the steady state during each period in IoT experiments. The 2.4 μA dynamic leakage current of the IPEHPM (which has also been confirmed by a Keithley source-meter) makes the IPEHPM an ultralow power consumption design with the total power consumption no larger than 4.2 V $\times$ 2.4 μA = 10.1 μW, which is much lower than 140 μW consumed by the MPPT control part alone in [21].

V. Conclusion

An IPEHPM has been developed for powering a low-power CO_2 IoT node at low illumination condition down to 200 lux. By ensuring the harvested energy is slightly larger than that application consumed, the energy storage efficiency of the IPEHPM will always be high enough for powering IoT node at indoor low illumination conditions even without adopting the commonly used dc–dc convertor and MPPT circuits which consume a considerable proportion of the energy harvested at low illuminations.

The IPEHPM has achieved 88.7% storage efficiency at 200 lux with over-charge and over-discharge protections ($\sim$10 μW power consumed by the entire IPEHPM at 200 lux). Its 3.6–4.2 V output voltage with 100 mA output current (up to 600 ms), makes the IPEHPM suitable for powering low-power IoT nodes. The IoT-based CO_2 concentration measurements for building ventilation provide a successful application example of using the IPEHPM for powering a low-power IoT node.

The newly developed indoor IPEHPM for building ventilation demonstrates that MPPT is not required when PV energy harvesting is employed as the primary power supply for continuous powering, which largely simplifies the power management to save power for ultralow-power IoT applications. The proposed PV energy-based power model with illumination parameter enables the utmost use of the PV energy for different illumination conditions. The measured in-circuit leakage current of supercapacitor (which was a missing key parameter for low-power design) enables supercapacitor's IoT applications.

References

[1] J. Bradley, J. Loucks, J. Macaulay, and A. Noronha, "Internet of everything (IoE) value index," Cisco, San Jose, CA, USA, White Paper, pp. 1–25, 2013.

[2] S. Puljarevic, "The interconnected world: A mega-market, *The Quintessence*, no. 13: Internet of Things, p. 3, 2013.

[3] S. Sudevalay and P. Kulkarui, "Energy harvesting sensor nodes: Survey and implications," *IEEE Commun. Surveys Tuts.*, vol. 13, no. 3, pp. 443–461, 2011.

[4] A. Klinefelter *et al.*, "A 6.45μW self-powered IoT SoC with integrated energy-harvesting power management and ULP asymmetric radios," in *Proc. IEEE Solid-State Circuits Conf.*, San Francisco, CA, USA, 2015, pp. 384–386.

[5] A. Al-Fuqaha, M. Guizani, M. Mohammadi, M. Aledhari, and M. Ayyash, "Internet of Things: A survey on enabling technologies, protocols, and applications," *IEEE Commun. Surveys Tuts.*, vol. 17, no. 4, pp. 2347–2376, 4th Quart., 2015.

[6] C. Perera, C. H. Liu, and S. Jayawardena, "The emerging Internet of Things marketplace from an industrial perspective: A survey," *IEEE Trans. Emerg. Topics Comput.*, vol. 3, no. 4, pp. 585–598, Dec. 2015.

[7] S. D. T. Kelly, N. K. Suryadevara, and S. C. Mukhopadhyay, "Towards the implementation of IoT for environmental condition monitoring in homes," *IEEE Sensors J.*, vol. 13, no. 10, pp. 3846–3853, Oct. 2013.

[8] *Annual Energy Review*, document DOE/EIA-0384(2009), U.S. Dept. Energy, Washington, DC, USA, Aug. 2010.

[9] J. Lu, A. Y. Kovalgi, K. H. M. van der Werf, R. E. I. Schropp, and J. Schmitz, "Integration of solar cells on top of CMOS chips part I: A-Si solar cells," *IEEE Trans. Electron Devices*, vol. 58, no. 7, pp. 2014–2021, Jul. 2011.

[10] A. M. Imtiaz, F. H. Khan, and H. Kamath, "All-in-one photovoltaic power system: Features and challenges involved in cell-level power conversion in ac solar cells," *IEEE Ind. Appl. Mag.*, vol. 19, no. 4, pp. 12–23, Jul./Aug. 2013.

[11] E. G. Fong *et al.*, "Integrated energy-harvesting photodiodes with diffractive storage capacitance," *IEEE Trans. Very Large Scale Integr. (VLSI) Syst.*, vol. 21, no. 3, pp. 486–497, Mar. 2013.

[12] D. Gibson and C. MacGregor, "A novel solid state non-dispersive infrared CO_2 gas sensor compatible with wireless and portable deployment," *Sensors*, vol. 13, no. 6, pp. 7079–7103, 2013.

[13] I. Mathews, G. Kelly, P. J. King, and R. Frizzell, "GaAs solar cells for indoor light harvesting," in *Proc. IEEE 40th Photovolt. Specialist Conf. (PVSC)*, Denver, CO, USA, 2014, pp. 0510–0513.

[14] H. G. Lee and N. Chang, "Powering the IoT: Storage-less and converter-less energy harvesting," in *Proc. 20th Asia South Pacific Design Autom. Conf.*, 2015, pp. 124–129.

[15] Y. Diab, P. Venet, H. Gualous, and G. Rojat, "Self-discharge characterization and modeling of electrochemical capacitor used for power electronics applications," *IEEE Trans. Power Electron.*, vol. 24, no. 2, pp. 510–517, Feb. 2009.

[16] M. Ayadi, A. Eddahech, O. Briat, and J.-M. Vinassa, "Voltage and temperature impacts on leakage current in calendar ageing of supercapacitors," in *Proc. 4th Int. Conf. Power Eng. Energy Elect. Drives*, Istanbul, Turkey, 2013, pp. 1466–1470.

[17] W. Wang *et al.*, "Super-capacitor and thin film battery hybrid energy storage for energy harvesting applications," *J. Phys. Conf. Series*, vol. 476, 2013, Art. no. 012105, doi: 10.1088/1742-6596/476/1/012105.

[18] A. S. Weddell, G. V. Merrett, and B. M. Al-Hashimi, "Photovoltaic sample-and-hold circuit enabling MPPT indoors for low-power systems," *IEEE Trans. Circuits Syst. I, Reg. Papers*, vol. 59, no. 6, pp. 1196–1204, Jun. 2012.

[19] X. Liu and E. Sánchez-Sinencio, "An 86% efficiency 12 μW self-sustaining PV energy harvesting system with hysteresis regulation and time-domain MPPT for IOT smart nodes," *IEEE J. Solid-State Circuits*, vol. 50, no. 6, pp. 1424–1437, Jun. 2015.

[20] S. Kim, K.-S. No, and P. H. Chou, "Design and performance analysis of supercapacitor charging circuits for wireless sensor nodes," *IEEE J. Emerg. Sel. Top. Circuits Syst.*, vol. 1, no. 3, pp. 391–402, Sep. 2011.

[21] Y. Wang *et al.*, "Storage-less and converter-less photovoltaic energy harvesting with maximum power point tracking for Internet of Things," *IEEE Trans. Comput.-Aided Design Integr. Circuits Syst.*, vol. 35, no. 2, pp. 173–186, Feb. 2016.

[22] X. Liu and E. Sánchez-Sinencio, "A highly efficient ultralow photovoltaic power harvesting system with MPPT for Internet of Things smart nodes," *IEEE Trans. Very Large Scale Integr. (VLSI) Syst.*, vol. 23, no. 12, pp. 3065–3075, Dec. 2015.

[23] W. Jung *et al.*, "An ultra-low power fully integrated energy harvester based on self-oscillating switched-capacitor voltage doubler," *IEEE J. Solid-State Circuits*, vol. 49, no. 12, pp. 2800–2811, Dec. 2014.

[24] D. Bol, E. H. Boufouss, D. Flandre, and J. De Vos, "A 0.48mm^2 5uW-10mW indoor/outdoor PV energy-harvesting management unit in a 65nm SoC based on a single bidirectional multi-gain/multi-mode switched-cap converter with supercap storage," in *Proc. 41st Eur. Solid-State Circuits Conf. (ESSCIRC)*, Graz, Austria, 2015, pp. 241–244.

[25] B. Martinez, M. Montón, I. Vilajosana, and J. D. Prades, "The power of models: Modeling power consumption for IoT devices," *IEEE Sensors J.*, vol. 15, no. 10, pp. 5777–5789, Oct. 2015.

[26] A. Nasiri, S. A. Zabalawi, and G. Mandic, "Indoor power harvesting using photovoltaic cells for low-power applications," *IEEE Trans. Ind. Electron.*, vol. 56, no. 11, pp. 4502–4509, Nov. 2009.

Xicai (Alex) Yue (M'14–SM'15) received the B.Eng. degree in telecommunication engineering and M.Eng. and Ph.D. degrees in biomedical engineering from Xi'an Jiaotong University, Xi'an, China, in 1985, 1995, and 1999, respectively.

He was a University Teaching Assistant and then a Lecturer teaching digital switching in China. From 1999 to 2016, he was with Tsinghua University, Beijing, China, Oxford Brookes University, Oxford, U.K., Imperial College London, London, U.K., and Sharp Laboratories of Europe, Oxford. He is currently a Senior Lecturer of bio-instrumentation and sensor interfacing with the University of the West of England, Bristol, U.K. His research experiences include digital switching, signal processing for otoacoustic emission and for auditory brainstem responses, pattern recognition with neural networks for speaker identification, sensor interfacing and data acquisition for stem cell cultures, medical imaging data acquisition (electrical impedance tomography for respiratory monitoring in intensive care, TFT process IC design for both ultrasound and single photon counting digital X-ray), real-time evaluation of human traumatic brain injury recovery process, implantable neural recordings for tiny insects as well as MEMs digital speakers. He has authored or co-authored over 20 peer-reviewed journal papers (as lead author) and a book chapter. His current research interests include active dry-electrodes for physiological measurements, low-power mixed-signal CMOS IC design for biomedical and wearable bio-sensing applications, and zero-power communication in wireless sensor networks/Internet of Things for building automation and home healthcare.

Dr. Yue was a recipient of the Live Demo Special Session Award of the IEEE International Symposium on Circuits and Systems in 2007.

Matthias Kauer (M'97–SM'13) received the Ph.D. degree in physics from the University of Cambridge, Cambridge, U.K., in 2000.

From 2001 to 2002, he was a Technical Staff Member with Bell Laboratories, Holmdel, NJ, USA. From 2003 to 2017, he was with Sharp Laboratories of Europe, Oxford, U.K., where he was a Research and Development Manager with Energy and Environment Technology. Since 2017, he has been with Lightricity Ltd., Oxford, which he co-founded. He has authored or co-authored over 40 journal papers and holds 15 patents. His current research interests include semiconductor optoelectronic devices, energy harvesting technologies, and applications of battery storage technology.

Mathieu Bellanger received the Physics and Engineering degree from the French "Grande école" Institut National des Sciences Appliquées, Toulouse, France, and the master's degree in nanophysics from the University of Paul Sabatier, Toulouse.

From 2008 to 2017, he was with the Sharp Laboratories of Europe, Oxford, U.K., where he was a Senior Researcher/Project Lead, involved with research on various projects covering a wide range of photovoltaic device technologies for flat plate, CPV, space, and Internet of Things applications. As one of the main inventors of the energy harvester, he has led the development and prototyping of this technology and successfully transferred it to mass manufacturing facilities. Since 2017, he has been with Lightricity Ltd., Oxford, which he co-founded.

Oliver Beard received the M.Eng. degree in electronic engineering from the University of Warwick, Coventry, U.K., in 2014.

From 2014 to 2016, he was a Graduate Researcher with Sharp Laboratories of Europe, Oxford, U.K., and became a Research Scientist in 2016. Since 2017, he has been a Research Scientist with Sharp Life Science (EU) Ltd., Oxford, as a Thin-Film Transistor Design Engineer for a bio-medical device. His current research interests include designing MEMS membrane systems and bio-medical TFT systems.

Mr. Beard was a recipient of the Dean's Award for Academic Excellence at the University of Warwick.

Mike Brownlow, photograph and biography not available at the time of publication.

Des Gibson received the B.Sc. (First Class Hons.) degree in physics and Ph.D. degree in thin film optics from the Queen's University at Belfast, Belfast, U.K.

He has a 30-year track record in industry, academic-based research and development and successful physics-based product commercialization, gained globally with Technical and Managing Director roles within blue chip organizations, small to medium sized companies, start-ups and close associations with academia. He has co-founded four successful physics-based technology companies focusing on thin film and sensor technologies. Two most recent are Gas Sensing Solutions Ltd., Glasgow, U.K., co-founded in 2006, and Applied Multilayers Ltd., Battle Ground, WA, USA, co-founded in 2002, and acquired 2010 by Telemark Inc., Battle Ground, WA, USA. Motivated by fresh challenges and a desire to focus on research, in 2014, he joined the University of the West of Scotland (UWS), Paisley, U.K., as a Professor of thin film and sensor technologies, where he is a founder and the Director of Research with the Institute of Thin Films, Sensors and Imaging. He is a named inventor on 16 patents with over 100 technical publications concerning thin films, sensors, and optoelectronics.

Dr. Gibson was a recipient of the United Kingdom Institute of Physics Innovation Award 2014. He is a Chartered Engineer and a Physicist. He is a Fellow of the Institute of Physics and a Senior Member of the Optical Society of America. He is a Principal Investigator of a new company spin out from UWS, researching and commercializing a novel miniaturized infrared spectrophotometer.

Caspar Clark, photograph and biography not available at the time of publication.

Calum MacGregor, photograph and biography not available at the time of publication.

Shigeng Song is a Senior Research Scientist with 25 years' experience in thin film physics and applications in optical coatings, sensors and flexible electronics, including material and process development, characterization, simulation, and device design. As a PI/CoI, he is currently involved with research on several projects for optical thin film devices, sensors and hyperspectral imaging funded by Innovate U.K., Swindon, U.K., BBSRC, Swindon, Scottish Enterprise, and Royal Society of Engineering, London, U.K. He has 3 U.K. patents, 3 Chinese patents, and over 50 papers. His current research interests include specific optical devices, sensitive materials, modeling and simulation for gas sensing, and hyperspectral imaging such as linear variable filters for miniaturized mid-IR spectrometers for multigas and chemical detection. In addition, he has had significant experience in sensor research and manufacturing, as well as industrial experiences in sensing and control applications including circuit board design and programming (VB6, C++, Mathcad, and MASM).